CHINESE OPTICS LETTERS

Vol. 20, No. 1 | January 2022

Post-treatment of 351 nm SiO_2 antireflective coatings for high power laser systems prepared by the sol-gel method

Bin Shen (沈 斌)[1*], Huai Xiong (熊 怀)[1**], Xu Zhang (张 旭)[1], Zhiya Chen (陈知亚)[1], Xiangyang Pang (庞向阳)[1], Yajing Guo (郭亚晶)[1], Chengjie Liang (梁成杰)[1,2], and Haiyuan Li (李海元)[1]

[1] Key Laboratory of High Power Laser and Physics, Shanghai Institute of Optics and Fine Mechanics, Chinese Academy of Sciences, Shanghai 201800, China

[2] Center of Materials Science and Optoelectronics Engineering, University of Chinese Academy of Sciences, Beijing 100049, China

*Corresponding author: bingo2011@siom.ac.cn

**Corresponding author: xhuai1998@siom.ac.cn

Received May 28, 2021 | Accepted August 17, 2021 | Posted Online September 28, 2021

Different post-treatment processes involving the use of ammonia and hexamethyldisilazane (HMDS) were explored for application to 351 nm third harmonic generation SiO_2 antireflective (3ω SiO_2 AR) coatings for high power laser systems prepared by the sol-gel method. According to experimental analysis, the 3ω SiO_2 AR coatings that were successively post-treated with ammonia and HMDS at 150°C for 48 h and again heat-treated at 180°C for 2 h (N/H 150 + 180 AR) were relatively better. There were relatively fewer changes in the optical properties of the N/H 150 + 180 AR coating under a humid and polluted environment, and the increase in defect density was slow in high humidity environments. The laser-induced damage threshold of the N/H 150 + 180 AR coating reached 15.83 J/cm^2 (355 nm, 6.8 ns), a value that meets the basic requirements of high power laser systems.

Keywords: optical materials; antireflection coatings; sol-gel; optics at surfaces; laser damage; thin films; optical properties.

DOI: 10.3788/COL202220.011601

1. Introduction

The sol-gel method, which was first, to the best of our knowledge, described by Ebelmen in 1846, has since been widely used to prepare different kinds of materials[1]. Porous silica antireflective (AR) coatings prepared using the sol-gel method possess excellent optical properties and superior laser-induced damage thresholds (LIDTs) and are typically used in final optics assemblies of inertial confinement fusion (ICF) experimental devices such as the National Ignition Facility (NIF) in the USA[2], Laser Mégajoule (LMJ) in France[3], and Shenguang facilities (SGs) in China[4–7]. Silicon oxide coatings with low refractive indices and prepared using the sol-gel method can be used for fused silica and crystal elements in final optics assemblies, while hafnium oxide and tantalum oxide coatings with high refractive indices can be used in reflective elements[8–10]. Unlike coatings prepared using physical vapor deposition (PVD), the sol-gel coating coated on optical elements has a high LIDT because of its high porosity and specific surface area[11]. The sol-gel method is also simple, convenient, and flexible for preparing coatings compared to PVD. Currently, numerous third harmonic generation (3ω) silica AR coatings coated on optical elements (such as fused silica, crystal optics, and disposable debris shields) are mainly used in the final optics assemblies of high power laser devices[12]. However, the performance stability of 3ω AR coatings will affect the final output quality of high power laser systems (HPLSs). Typically, the 3ω AR coatings for the glass optics of HPLSs are post-treated for a specific duration in a chemical atmosphere with fluorine or long-carbon-chain reagents to improve their performance stabilities[13–15]. Most studies focus on the stability of optical properties, such as the transmittance decrease of AR coatings at 3ω wavelength; however, the formation of coating defects is ignored in the accelerated experiment, and the number of defects may affect the damage to the downstream optical elements[16]. Therefore, it is necessary to investigate post-treatment processes for 3ω AR coatings that can be applied to HPLSs.

After studying the post-treatment processes for 3ω AR coatings used in different HPLSs, including NIF, LMJ, and SG II[17–19], in this study, the effects of four different post-treatment processes on 3ω AR coatings were investigated by analyzing the coating transmittances in high temperature, high humidity, and organic contaminated environments, coating defects in a high humidity environment, and LIDTs. In the post-treatment process, 3ω SiO_2 AR coatings that were successively post-treated with ammonia and hexamethyldislazane (HMDS) at 150°C for 48 h separately

and again heat-treated at 180°C for 2 h (N/H 150 + 180 AR) are relatively better in both optical stability and defect control.

2. Experiments

The SiO_2 sol was prepared using purified tetraethoxysilane (TEOS), ammonia ($NH_3 \cdot H_2O$), ethanol (EtOH), and polyethylene glycol (PEG200). The molar ratio of the chemical reagents in the solution was TEOS:EtOH:NH_3:H_2O = 1:34.2:0.9:2, and a certain amount of PEG200 was added. After stirring the solution in ice water for a specific duration, the sealed solution was aged for some days in an oven set to 50°C. The solution was then refluxed to remove excess $NH_3 \cdot H_2O$ until the pH of the SiO_2 sol was seven. Finally, the 3ω sol used for the 3ω AR coating via dip coating was obtained by diluting the initial SiO_2 sol with a certain amount of EtOH.

The JGS1 (far ultraviolet silica fused glass, transparent in the range of ultraviolet and visible spectra) substrates with a diameter and thickness of 32 and 7 mm, respectively, were completely immersed in the 3ω sol at a speed of 5–10 cm/min. The substrates were then pulled out at the same speed using a custom-made dip coating machine. The actual coating process usually needs to test the peak wavelength (λ) of coating transmittance and adjust the dip coating speed. After the JGS1 substrates with AR coatings were placed in a drying cabinet for more than 2 h, they were heat-treated in an oven at 180°C for 24 h to obtain a heat-treated 3ω AR coating (JGS1 with 3ω AR) whose optical thickness ($\lambda/4$) is about 88 nm.

All of the JGS1 samples with 3ω AR coatings were post-treated via different processes in a chemical atmosphere, as shown in Fig. 1. Two beakers containing approximately 30 mL each of $NH_3 \cdot H_2O$ and HMDS were heated in an oven at 150°C for 48 h to constitute two different post-treatment processes [two steps (1, 2) and one step (3, 4)]. Finally, JGS1 substrates 1 and 3 were heat-treated for another 2 h at 180°C.

3. Results and Discussion

Typically, the refractive index of silica AR coatings is approximately 1.20, and coating elements with excellent AR performance for 3ω can be obtained and applied to the final output main optical path of HPLSs by matching the refractive index of the AR coating with that of the element. However, due to the porous nature of the sol-gel silica coating, the coating elements, when used in laser devices for a long time, are mainly affected by the experimental environment, such as water vapor in air and contaminants in the devices. Typically, the stability of the silica coatings will decrease under such environmental conditions over time. The stability performance of silica coatings can be determined by their optical properties, contact angles, and surface defects.

Samples 1–4 were placed in the high temperature, high humidity Espec LH-213 oven for 24 h, where the temperature and relative humidity of the oven were set to 85°C and 85% (85°C/85 RH), respectively. The changes in the performance of the coating were determined under extreme temperature and humidity conditions to simulate experimental conditions. The transmittances of samples 1–4 under different experimental conditions were tested using a Lambda900 spectrophotometer (PerkinElmer, USA). The optical performances of samples 1–4 at different experimental stages are illustrated in Fig. 2; note that the testing range for spectrophotometry was 200–800 nm. The peak transmittance (T_{max}) and wavelength (λ_{max}) of the corresponding samples are shown in Table 1. Figure 2 indicates that all samples undergo a slight red shift at the peak transmittance after post-treatment because the hydrophobic trimethyl groups are attached to the surface of the silica coating after post-treatment. Samples 1 and 3 exhibit similar peak transmittances before and after post-treatment, while samples 2 and 4 exhibit peak transmittances reduced by 0.15% and 0.21%, respectively, after post-treatment; and the peak wavelength of samples 2 and 4 red shifted about 20 nm. In the post-treatment process, the gasification of $NH_3 \cdot H_2O$ and HMDS created a sealed oven to form a chemical atmosphere. The HMDS gas perhaps gradually liquefied to form microbeads that blocked the pores of the silica coating when the oven temperature was decreased; this increased the refractive

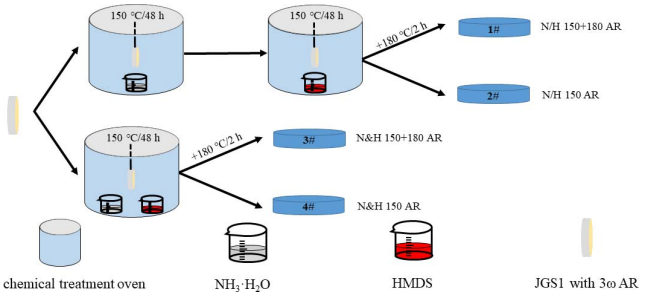

Fig. 1. Schematic diagram showing post-treatment processes of 3ω AR.

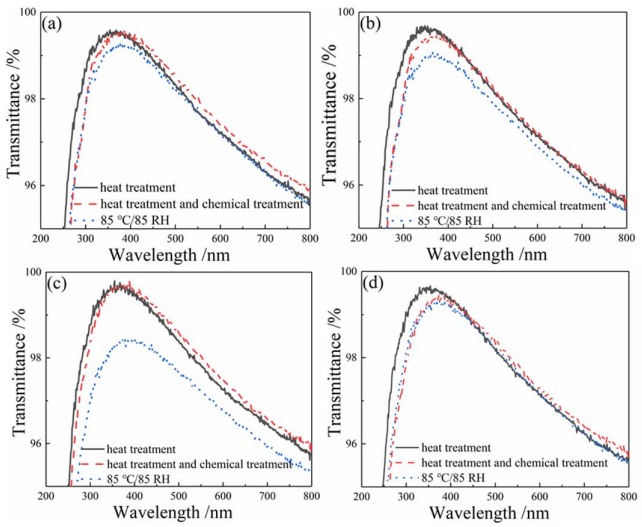

Fig. 2. Optical performance of 3ω AR coatings at different experimental stages: (a) sample 1, (b) sample 2, (c) sample 3, (d) sample 4.

Table 1. Peak Transmittance and Wavelength of 3ω AR Coatings at Different Experimental Stages.

	Effect of Heat Treatment		Effect of Heat Treatment and Post-Treatment		Effect of 85°C/85 RH	
Sample	λ_{max}/nm	T_{max}/%	λ_{max}/nm	T_{max}/%	λ_{max}/nm	T_{max}/%
1	368	99.58	374	99.55	376	99.28
2	355	99.65	373	99.50	372	99.03
3	366	99.65	369	99.67	388	98.42
4	354	99.67	374	99.46	372	99.25

index of the silica coating and decreased the transmittance of the element. The microbeads in the porous silica coating were discharged by another round of heat treatment in an oven at 180°C for 2 h. At the same time, the peak wavelengths of the samples did not exhibit a noticeable shift after 85°C/85 RH environment, while the peak transmittance of the samples decreased in general and the peak transmittance of sample 1 after 85°C/85 RH environment was the highest (99.28%) among all the samples. This indicates that the water molecules infiltrated the pores of the silica coatings, leading to a decrease in the peak transmittance. The lower decrease in the peak transmittance of sample 1 may be because the surface of the silica coating subjected to the two-step post-treatment reacted more efficiently with $NH_3 \cdot H_2O$ and HMDS than that of the coating subjected to the one-step post-treatment and because the surfaces of the silica coatings were covered with hydrophobic groups.

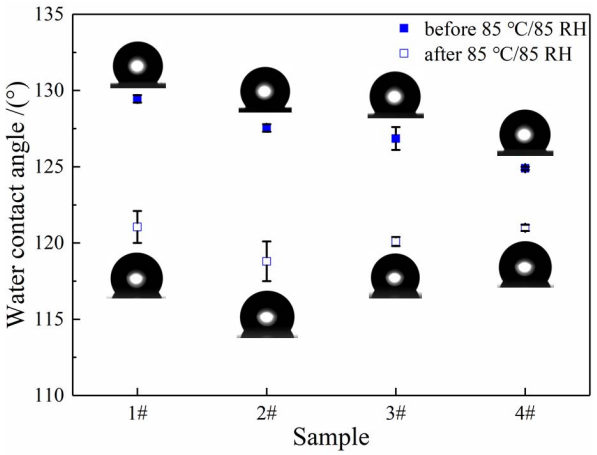

Fig. 3. Water contact angles of the 3ω AR coatings.

The water contact angles of the silica coatings after post-treatment and 30 days after the end of the high temperature, high humidity experiment were measured using the optical contact angle (OCA) 40 system (Dataphysics Instruments, Germany); the results are shown in Fig. 3. For the test, 3 μL deionized water droplets were used, and the coating was in contact with the water droplet for 10 s before being sampled. Hydrophobic groups were formed on the surface of the silica coatings, resulting in good hydrophobic properties after post-treatment. All four samples exhibited contact angles greater than 125° between the silica coating and water droplet; the contact angle of sample 1 was close to 130°, indicating excellent hydrophobic properties. The water contact angles of all samples were maintained at approximately 120° after testing under extreme conditions, which showed that different post-treatment

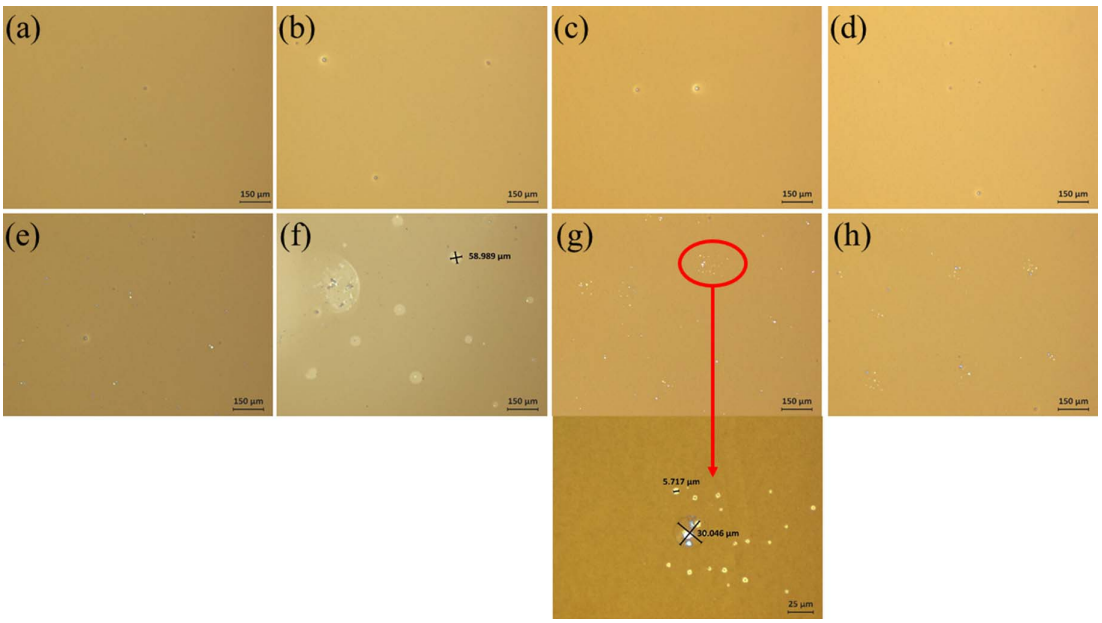

Fig. 4. Defect positions of all samples. (a)–(d) samples 1–4 before 85°C/85 RH treatment, (e)–(h) samples 1–4 after 85°C/85 RH treatment.

processes can induce better hydrophobicity on the surface of silica coatings.

The basis of the coating stability was the stability of the coating transmittance and hydrophobicity; however, changes in the surface defects of silica coatings will eventually affect the LIDT of the silica coating[20]. The defect situations in all samples before and after 85°C/85 RH conditions were observed using a DM4000 metallurgical microscope (Leica, Germany), as illustrated in Fig. 4. There were few defects observed on the coating surface as seen in the 1.3 mm^2 field of the microscope before the 85°C/85 RH experiment, and the sizes of the defects were approximately 15 μm. However, more defects with different characteristics were observed on the surface coating of each sample after the 85°C/85 RH experiment. Among them, the defect features of samples 1 and 2 were single defect points, but the defect points of sample 2 affected the surrounding areas with a diameter of approximately 60 μm. The defect features of samples 3 and 4 were cluster defect points dispersed around the main defect point, which greatly increased the defect density of the silica coating. Numerous defects that appeared may affect the damage resistance of the coatings and progress of the experiments. Sample 1 with the two-step post-treatment process has good stability of defect growth. It is because the first step with $NH_3 \cdot H_2O$ not only forms Si-O-Si bond and then strengthens the SiO_2 spherical framework on the coating, but also partially replaces the Si-OC_2H_5 bond with a Si-OH bond, which is conducive to the next reaction with HMDS to form Si-$(CH_3)_3$[21]. Compared to sample 2, after sample 1 was heated at 180°C/2 h again, perhaps some amount of HMDS droplets in the coating pores vaporized and some formed new Si-CH_3 bonds in the pores, which also may increase the stability of sample 1.

The particulate contaminants from motors, lubricants, and organic plasticizers are volatilized inside the vacuum components during experimentation with HPLSs, which will also affect the properties of the sol-gel coatings[22]. An off-line experiment

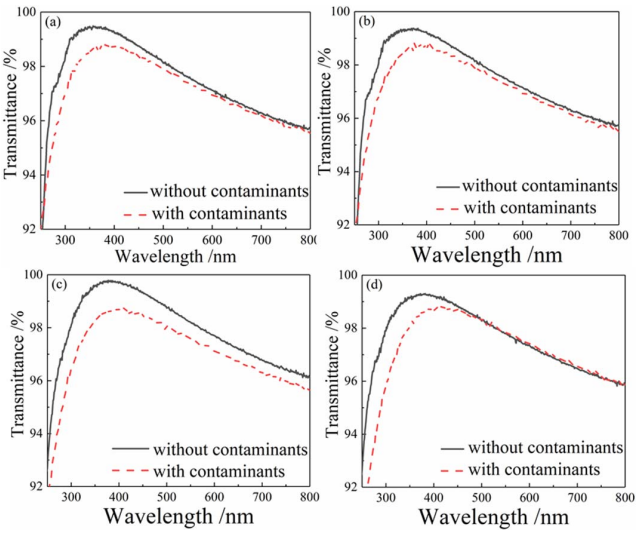

Fig. 5. Transmittance spectra before and after contamination: (a) sample 1, (b) sample 2, (c) sample 3, (d) sample 4.

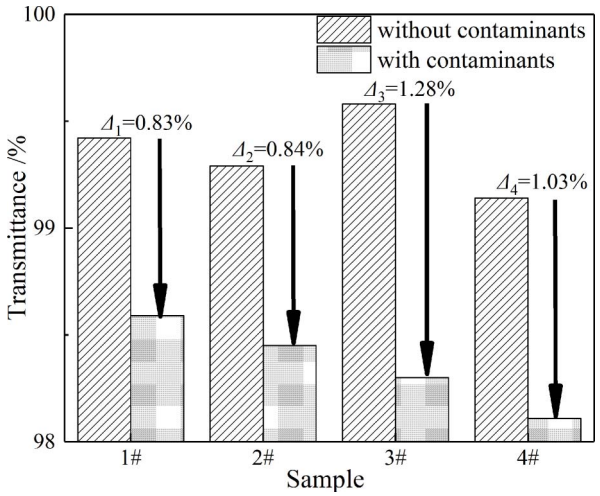

Fig. 6. Transmission loss of samples at 351 nm.

simulated hydrocarbon volatilization in a vacuum chamber, which was found to influence the sol-gel coating. The temperature of the vacuum chamber was increased from 22°C to 50°C, and the pressure was varied from atmospheric vacuum to 10^{-6} Torr. These conditions were maintained for 1 h, followed by slow cooling to 22°C before the pressure returned to normal after 3 h. The hydrocarbon contamination source in the volatile cavity was a 1.0 mg mixture of 85% squalene ($C_{30}H_{62}$) and 15% dioctylphthalate ($C_{24}H_{38}O_4$)[17]. Figure 5 shows the transmittance spectra of all samples before and after contamination, and Figure 6 shows the transmission loss (Δ) of the samples at 351 nm after exposure to hydrocarbons. The peak transmittances of all samples noticeably decreased, and the peak wavelengths shifted after hydrocarbon volatilization in a 50°C vacuum environment. In comparison, the transmission losses at 351 nm for samples 1 and 2 were lower after the contamination.

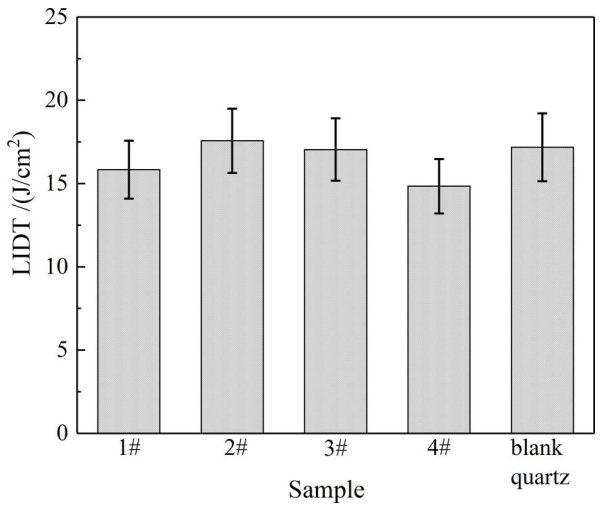

Fig. 7. LIDT (355 nm, 6.8 ns) results of the samples.

The defects in the optical coatings were the main source of damage under long-pulse laser irradiation[23,24]. The LIDTs of the elements with a coating were recorded using the small-sized LIDT test platform at the Shanghai Institute of Optics and Fine Mechanics by the "1-on-1" method. The test results are shown in Fig. 7. The wavelength of the laser used in the test was 355 nm, and the full width at half-maximum was 6.8 ns. To apply the coated components to HPLSs, the LIDTs of the most recently developed coated components must meet the basic requirements. It was observed that the LIDTs of the samples were close to each other. Specifically, the LIDTs reached 14.84–17.57 J/cm^2, and those of samples 1–3 were slightly higher than those of sample 4, which is currently used in the SG II laser facility.

4. Conclusion

In conclusion, post-treatment is an important process in preparing sol-gel coatings for optical elements. This study aimed to optimize the post-treatment process for sol-gel SiO_2 coatings using experiments that can be applied to HPLSs. The comprehensive performance of 3ω SiO_2 AR coatings with the post-treatment process of N/H 150 + 180 AR was the most efficient in terms of the parameters tested (i.e., transmittance, defect density, water contact angle, and LIDT).

Acknowledgement

This work was supported by the Strategic Priority Research Program of Chinese Academy of Sciences (No. XDA25020305).

References

1. E. Ebelmen, "Researches sur les combinaisons des acides borique et silicique avecles ethers," Ann. Chim. Phys. **16**, 129 (1846).
2. J. H. Campbell, R. Hawley-Fedder, C. J. Stolz, J. A. Menapace, M. R. Borden, P. Whitman, J. Yu, M. Runkel, M. Riley, M. Feit, and R. Hackel, "NIF optical materials and fabrication technologies: an overview," Proc. SPIE **5341**, 84 (2004).
3. P. Belleville, P. Prene, C. Bonnin, L. Beaurain, and Y. Montouillout, "How smooth chemistry allows high power laser optical coating preparation," Proc. SPIE **5250**, 196 (2004).
4. R. J. Liu, R. Y. Zhan, Y. X. Tang, and J. Q. Zhu, "A moisture-resistant antireflective coating by sol-gel process for neodymium-doped phosphate laser glass," Chin. Opt. Lett. **4**, 119 (2006).
5. Y. Wei, H. B. Lü, X. D. Jiang, C. Tang, H. Ren, and K. Li, "Fabrication of broadband antireflective films by sol-gel spin-coating process for high power lasers," High Power Laser Particle Beams **15**, 647 (2003).
6. J. Q. Zhu, "Review of special issue on high power facility and technical development at the NLHPLP," High Power Laser Sci. Eng. **7**, e12 (2019).
7. F. Suzuki-Vidal, T. Clayson, C. Stehle, U. Chaulagain, J. W. D. Halliday, M. Y. Sun, L. Ren, N. Kang, H. Y. Liu, B. Q. Zhu, J. Q. Zhu, C. D. Rossi, T. Mihailescu, P. Velarde, M. Cotelo, J. M. Foster, C. N. Danson, C. Spindloe, J. P. Chittenden, and C. Kuranz, "First radiative shock experiments on the SG-II laser," High Power Laser Sci. Eng. **9**, e27 (2021).
8. H. Xiong, Y. X. Tang, L. L. Hu, and H. Y. Li, "An ORMOSIL porous double-layer broadband antireflective coating," Chin. Opt. Lett. **17**, 112201 (2019).
9. M. G. Blanchin, B. Canut, Y. Lambert, V. S. Teodorescu, A. Barau, and M. Zaharescu, "Structure and dielectric properties of HfO_2 films prepared by a sol–gel route," J. Sol-Gel Sci. Technol. **47**, 165 (2008).
10. P. Belleville, P. Prené, and B. Lambert, "UV-cured sot-gel broadband antireflective and scratch-resistant coating for CRT," Proc. SPIE **3943**, 67 (2000).
11. Y. J. Guo, X. T. Zu, X. D. Jiang, X. D. Yuan, W. G. Zheng, S. Z. Xu, and B. Y. Wang, "Laser-induced damage mechanism of the sol–gel single-layer SiO_2 acid and base thin films," Nucl. Instrum. Methods Phys. Res. B **266**, 3190 (2008).
12. M. L. Spaeth, K. R. Manes, D. H. Kalantar, P. E. Miller, J. E. Heebner, E. S. Bliss, D. R. Speck, T. G. Parham, P. K. Whitman, P. J. Wegner, P. A. Baisden, J. A. Menapace, M. W. Bowers, S. J. Cohen, T. I. Suratwala, J. M. Di Nicola, M. A. Newton, J. J. Adams, J. B. Trenholme, R. G. Finucane, R. E. Bonanno, D. C. Rardin, P. A. Arnold, S. N. Dixit, G. V. Erbert, A. C. Erlandson, J. E. Fair, E. Feigenbaum, W. H. Gourdin, R. A. Hawley, J. Honig, R. K. House, K. S. Jancaitis, K. N. LaFortune, D. W. Larson, B. J. Le Galloudec, J. D. Lindl, B. J. MacGowan, C. D. Marshall, K. P. McCandless, R. W. McCracken, R. C. Montesanti, E. I. Moses, M. C. Nostrand, J. A. Pryatel, V. S. Roberts, S. B. Rodriguez, A. W. Rowe, R. A. Sacks, J. T. Salmon, M. J. Shaw, S. Sommer, C. J. Stolz, G. L. Tietbohl, C. C. Widmayer, and R. Zacharias, "Description of the NIF laser," Fusion Sci. Technol. **69**, 25 (2016).
13. S. D. Wang and Y. Y. Shu, "Superhydrophobic antireflective coating with high transmittance," J. Coat. Technol. Res. **10**, 527 (2013).
14. Q. H. Zhang, W. Yang, H. J. Ma, P. Ma, and Q. Xu, "Modification of porous silica antireflective coatings with fluorine-containing organosilicon," Acta Opt. Sin. **29**, 1719 (2009).
15. M. Y. Wei, X. M. Wang, S. G. Qing, Z. K. Luo, H. X. Zheng, and S. Q. Liu, "Preparation of KH560/KH570 modified SiO_2 antireflective coating," Mater. Rep. B **26**, 7 (2012).
16. M. V. Monticelli, M. C. Nostrand, N. Mehta, L. Kegelmeyer, M. A. Johnson, J. Fair, and C. Widmayer, "The HMDS coating flaw removal tool," Proc. SPIE **7132**, 71320V (2008).
17. D. S. Hobbs, B. D. Macleod, E. Sabatino, III, J. A. Britten, and C. J. Stolz, "Contamination resistant antireflection nano-textures in fused silica for laser optics," Proc. SPIE **8885**, 88850J (2013).
18. P. F. Belleville and H. G. Floch, "Ammonia hardening of porous silica antireflective coatings," Proc. SPIE **2288**, 25 (1994).
19. H. Y. Li and Y. X. Tang, "Study on stability of porous silica antireflective coatings prepared by sol-gel processing," Chin. J. Lasers **32**, 839 (2005).
20. C. L. Zhang, X. B. Li, H. B. Lü, X. D. Yuan, Z. G. Wang, and X. T. Zu, "Influence of impurities on laser-induced damage of sol-gel SiO_2 films," High Power Laser Particle Beams **23**, 1267 (2011).
21. I. M. Thomas, A. K. Burnham, J. R. Ertel, and S. C. Frieders, "Method for reducing the effect of environmental contamination of sol gel optical coatings," Proc. SPIE **3492**, 220 (1999).
22. X. Y. Pang, M. Y. Sun, Q. T. Fan, H. Xiong, C. Y. Wang, and Z. G. Liu, "Online detection of airborne molecular contamination and its influence on the sol-gel coating," Proc. SPIE **10748**, 107480Z (2018).
23. C. Shan, Y. A. Zhao, Y. Q. Gao, X. H. Zhao, G. H. Hu, W. X. Ma, and J. D. Shao, "Laser-induced defects in optical multilayer coatings by the spatial resolved method," Chin. Opt. Lett. **17**, 031403 (2019).
24. T. Y. Pu, W. W. Liu, Y. L. Wang, X. M. Pan, L. Q. Chen, and X. F. Liu, "A novel laser shock post-processing technique on the laser-induced damage resistance of 1ω HfO_2/SiO_2 multilayer coatings," High Power Laser Sci. Eng. **9**, e19 (2021).